

PMD tolerant direct-detection polarization division multiplexed OFDM systems with MIMO processing

Chia-Chien Wei,^{1*} Chun-Ting Lin,² and Chih-Yun Wang²

¹ Department of Photonics, National Sun Yat-sen University, Kaohsiung, Taiwan

² Institute of Photonic System, National Chiao Tung University, Tainan, Taiwan
*ccwei@mail.nsysu.edu.tw

Abstract: This work proposes a novel direct-detection polarization division multiplexed OFDM scheme without the need of dynamic polarization control at a polarization-diverse receiver, and the proposed scheme is robust against polarization mode dispersion. Setting the frequency difference between two polarization-orthogonal reference carriers as one subcarrier spacing, possible signal fading can be avoided, and the corresponding interference from adjacent subcarriers is eliminated by a novel MIMO algorithm. The penalty caused by high channel matrix condition number can be decreased by inserting empty tones among subcarriers, and the polarization-dependent OSNR penalty at the BER of 10^{-3} is <3.6 dB with an empty tone inserted every 8 subcarriers. Moreover, the numerical results demonstrate the 16×10^3 -ps/nm chromatic dispersion and the 300-ps differential group delay will not induce additional penalty.

©2012 Optical Society of America

OCIS codes: (060.2330) Fiber optics communications; (060.4080) Modulation.

References and links

1. Y. Ma, Q. Yang, Y. Tang, S. Chen, and W. Shieh, "1-Tb/s single-channel coherent optical OFDM transmission over 600-km SSMF fiber with subwavelength bandwidth access," *Opt. Express* **17**(11), 9421–9427 (2009).
2. S. L. Jansen, A. Al Amin, H. Takahashi, I. Morita, and H. Tanaka, "132.2-Gb/s PDM-8QAM-OFDM transmission at 4-b/s/Hz spectral efficiency," *IEEE Photon. Technol. Lett.* **21**(12), 802–804 (2009).
3. H. Takahashi, A. Al Amin, S. L. Jansen, I. Morita, and H. Tanaka, "Highly spectrally efficient DWDM transmission at 7.0 b/s/Hz using 8×65.1 -Gb/s coherent PDM-OFDM," *J. Lightwave Technol.* **28**(4), 406–414 (2010).
4. D.-Z. Hsu, C.-C. Wei, H.-Y. Chen, W.-Y. Li, and J. Chen, "Cost-effective 33-Gbps intensity modulation direct detection multi-band OFDM LR-PON system employing a 10-GHz-based transceiver," *Opt. Express* **19**(18), 17546–17556 (2011).
5. B. J. Schmidt, Z. Zan, L. B. Du, and A. J. Lowery, "120 Gbit/s over 500-km using single-band polarization-multiplexed self-coherent optical OFDM," *J. Lightwave Technol.* **28**(4), 328–335 (2010).
6. M. Mayrock and H. Haunstein, "PMD tolerant direct-detection optical OFDM system," in *Proc. ECOC'07* (2007), paper 5.2.5.
7. W.-R. Peng, K.-M. Feng, and A. E. Willner, "Direct-detected polarization division multiplexed OFDM systems with self-polarization diversity," in *Proc. CLEOS'08* (2008), paper MH3.
8. D. Qian, N. Cvijetic, J. Hu, and T. Wang, "108 Gb/s OFDMA-PON with polarization multiplexing and direct detection," *J. Lightwave Technol.* **28**(4), 484–493 (2010).
9. A. Amin, H. Takahashi, I. Morita, and H. Tanaka, "100-Gb/s direct-detection OFDM transmission on independent polarization tributaries," *IEEE Photon. Technol. Lett.* **22**(7), 468–470 (2010).
10. C.-T. Lin, C.-C. Wei, and M.-I. Chao, "Phase noise suppression of optical OFDM signals in 60-GHz RoF transmission system," *Opt. Express* **19**(11), 10423–10428 (2011).
11. W.-R. Peng, "Analysis of laser phase noise effect in direct-detection optical OFDM transmission," *J. Lightwave Technol.* **28**(17), 2526–2536 (2010).
12. A. J. Lowery, "Improving sensitivity and spectra efficiency in direct-detection optical OFDM systems," in *Proc. OFC'08*. (2008), paper OMM4.

1. Introduction

Due to the exponentially growing demand for various broadband services, a high-capacity solution to next-generation optical networks must be spectrally efficient. Thanks to the advancement of digital signal processing (DSP), combined with spectrally efficient quadrature amplitude modulation (QAM), chromatic dispersion (CD) tolerant optical orthogonal frequency-division multiplexing (OFDM) has emerged as a potential candidate for future optical communication systems [1–9]. Although coherent (CO) OFDM can achieve high receiver sensitivity, narrow-linewidth lasers are required at the transmitter and the receiver, as well as frequency-offset and phase noise compensation algorithms [1–3]. By transmitting a reference optical carrier along with the OFDM signal, direct-detection (DD) is an alternative scheme to realize optical OFDM transmission, and its receiver can get rid of an optical hybrid and a local oscillator [4–9].

With a polarization-diverse receiving scheme [2, 3] and multiple-input multiple-output (MIMO) processing, CO-OFDM can be combined with a polarization division multiplexed (PDM) technique to increase spectral efficiency, and it is robust to polarization mode dispersion (PMD). Nonetheless, DD-OFDM would require the reference carrier to be equally separated into two polarization-diverse detectors to realize the PDM scheme [5] and/or to avoid PMD-induced power fading [6]. Consequently, impractical dynamic polarization control is needed to adjust the state of polarization (SOP) of the co-propagated reference carrier. In [7], a self-polarization-diverse receiver utilizes a narrow-band filter and a Faraday rotator mirror to rotate the carrier's SOP alone by 90° . Then, the PDM-OFDM signals over orthogonal polarizations can be detected individually without polarization control. Nonetheless, the frequency of the narrow-band filter must be controlled precisely. Moreover, two orthogonal-orthogonal reference carriers are generated at different sidebands with respect to the PDM-OFDM signals [8, 9]. Hence, the OFDM signals can be demodulated by the polarization-diverse receiver and MIMO processing [8], or subcarriers at a specific SOP can be detected without MIMO processing by filtering out the unnecessary reference carrier [9]. However, these schemes require twice guard interval, and the polarization-orthogonality between the reference carriers would be destroyed by PMD.

This work proposes a novel DD-PDM-OFDM scheme, and the scheme is robust against PMD without the need of additional optical filter and polarization control. In this scheme, the frequency of one of the reference optical carriers is shifted by one subcarrier spacing. Hence, possible signal fading is prevented at the polarization-diverse receiver. Due to the different frequencies of the reference carriers, a novel MIMO algorithm is applied to remove the interference from adjacent subcarriers after photo-detection. However, the channel matrix of the MIMO algorithm has high condition number at some received SOP to result in performance penalty. To reduce the penalty, empty tones are inserted among subcarriers to decrease the condition number. From our numerical results, inserting an empty tone every 8 subcarriers can reduce the maximum polarization-dependent optical signal-to-noise ratio (OSNR) penalty at the bit-error rate (BER) of 10^{-3} to ~ 3.6 dB, and more empty tones would further decrease the penalty at the price of lower spectral efficiency. Furthermore, simulation is given to show the ability of the proposed scheme against CD and the first order PMD. With the CD of 16×10^3 ps/nm and the differential group delay (DGD) of 300 ps, 16-QAM 47-Gbps DD-PDM-OFDM signals suffer from negligible additional OSNR penalty.

2. Operation principle

While a polarization beam combiner (PBC) is applied to combine two DD-OFDM signals, x_1 and x_2 , in the PDM scheme, their reference carriers turn out to be one completely polarized carrier shown in Fig. 1(a). Hence, the reference carrier of the traditional DD-PDM-OFDM scheme could be generated directly in the form of single-polarization [5]. After transmission over polarization-uncontrolled channel, the traditional scheme requires dynamic polarization

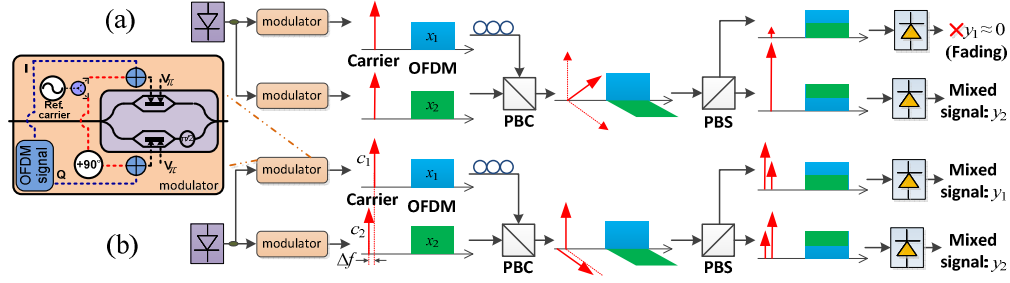


Fig. 1. The schematic plots of (a) the traditional DD-PDM-OFDM scheme without polarization control, and (b) the proposed scheme (inset: the setup of the modulator used in this work [10])

Since the beating term between the N^{th} subcarrier and the carrier of c_2 will become the $(N + 1)^{\text{th}}$ subcarriers, \mathbf{Y} and \mathbf{W} are $(2N + 2) \times 1$ vectors, and \mathbf{H} is a $(2N + 2) \times (2N)$ matrix. Moreover, the transmitted OFDM signals are assigned from the 1st to the N^{th} subcarriers, and therefore, \mathbf{h}_1 and \mathbf{h}_{N+1} in Eq. (2) are 2×2 matrices, instead of 2×4 matrices presented in Eq. (1). Once the channel response of \mathbf{h}_i is estimated by proper training symbols, the MIMO demodulation can be realized by the zero-forcing algorithm of $\mathbf{H}^{-1}\mathbf{Y}$, where \mathbf{H}^{-1} indicates the pseudo inverse of \mathbf{H} .

When the zero-forcing algorithm is applied, nonetheless, the recovered signals are composed of the transmitted signal \mathbf{X} and the noise term of $\mathbf{H}^{-1}\mathbf{W}$. Accordingly, the noise would be intensified, if the condition number of \mathbf{H} is high. Unfortunately, since N of an OFDM signal is generally large, the condition number of \mathbf{H} might be high. Without considering CD and PMD for simplicity, the optical channel could be treated as a frequency-irrelevant random orientated Jones matrix, \mathbf{R} , with the entries of r_{11} , r_{12} , r_{21} , and r_{22} . Figure 2(a) shows the corresponding relations among the transmitted and received optical signals. For example, $y_{1,i}$ will include $r_{11}r_{12}^*x_{1,i-1}c_2^*$ which is the beating term between $r_{11}x_{1,i-1}$ and $r_{12}c_2$. Hence, let the powers of both carriers be unity, the channel response, \mathbf{h}_i , can be represent as

$$\mathbf{h}_i = \begin{bmatrix} r_{11}r_{12}^* & |r_{12}|^2 & |r_{11}|^2 & r_{11}^*r_{12} \\ r_{21}r_{22}^* & |r_{22}|^2 & |r_{21}|^2 & r_{21}^*r_{22} \end{bmatrix} \quad (3)$$

When \mathbf{R} is diagonal or anti-diagonal indicating no polarization mixing, the condition number of \mathbf{H} is unit and irrelevant to N , and the powers of \mathbf{W} and $\mathbf{H}^{-1}\mathbf{W}$ will be identical. Nevertheless, if two orthogonal signals are equally separated into two receivers and $|r_{11}| = |r_{12}| = |r_{21}| = |r_{22}|$, the condition number and the power of $\mathbf{H}^{-1}\mathbf{W}$ will become the highest and increase with N . Because the condition number is independent of the relative phase among the entries of \mathbf{R} , \mathbf{R} can be assumed real and $r_{11} = r_{22} = \cos\theta$ and $r_{12} = -r_{21} = \sin\theta$, where θ can be understood as the relative angle between the PBC at the transmitter and the PBS at the receiver. Consequently, the best and the worst cases can be denoted by θ of 0 and 45° , respectively. Moreover, with a large N , the computational complexity of \mathbf{H}^{-1} would also be high for hardware implementation. Hence, to lower both the condition number of \mathbf{H} and the computational complexity of \mathbf{H}^{-1} , empty tones are required to separate subcarriers into groups shown in Fig. 2(b). When each group is composed of N_g subcarriers, the numbers of groups and empty tones are both N/N_g , and therefore, the spectral efficiency of the proposed scheme becomes $\sim 2 \times N_g/(1 + N_g)$ times, compared with a single-polarization DD-OFDM system.

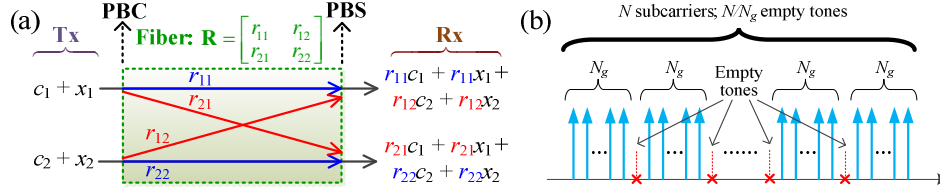


Fig. 2. The schematic plots of (a) the frequency-irrelevant Jones matrix of the channel and (b) allocating empty tones

3. Numerical results and discussion

In our simulation, a dual-parallel Mach-Zehnder modulator (MZM) is adopted, as shown in the inset of Fig. 1 [10], and the generation of each DD-OFDM signal requires only one MZM by electrically combining baseband OFDM signals and a sinusoidal wave. With respect to the laser frequency, the reference optical carriers are generated at the lower sideband, and the OFDM signal composed of 160 subcarriers are modulated at the baseband. All the subcarriers are encoded by random binary data as 16-QAM format with the fast-Fourier transform size of 256. With the sampling rate of 10 GSample/s and the CP of 1/16, the assemble data rates are 23.5 Gbps for each polarization and 47 Gbps for the DD-PDM-OFDM signal. The fiber transmission is assumed to be linear and lossless, and the transmission impairments of CD and the first order PMD are considered in our simulation. To evaluate the system performance in terms of OSNR, additive white Gaussian noise is loaded at both polarizations in front of the receiver to model amplified spontaneous emission (ASE) noise, and the out-of-band ASE noise is filtered by a 2nd order Gaussian filter with the 3-dB bandwidth of 30 GHz. Furthermore, the laser linewidth is set as 100 kHz to decrease the dispersion-induced phase noise [11], and the received OSNR is defined with the noise bandwidth of 0.1 nm.

Figure 3(a) shows the demodulated signal-to-noise ratios (SNRs) of each subcarrier for the best and the worst cases with the same OSNR of 24 dB and the N_g of 8 at back-to-back (BtB). In addition to the average SNR penalty of ~3.5 dB caused by polarization mixing, the subcarriers at the middle of each group show worse SNRs, compared with the subcarriers at the edge of each group which suffer the least interference from adjacent subcarriers. With N_g of 8, Fig. 3(b) plots the required OSNR to reach the BER of 10^{-3} as a function of θ at BtB, and the OSNR penalty caused by polarization mixing is smaller than 3.6 dB. Furthermore, Fig. 4(a) depicts the demodulated SNRs for the worst case with the same OSNR of 24 dB but different N_g of 8 and 40 at BtB. The subcarriers at the edges show similar SNRs for both cases, but for N_g of 40, those at the middle of each group suffer from the additional penalty of ~6 dB due to the higher condition number. Besides, the required OSNR for the BER of 10^{-3} is plotted in Fig. 4(b) with different N_g . While the required OSNRs for the case without polarization mixing are irrelevant to N_g , the required OSNRs of the worst cases will increase with N_g . In addition, the power of the beating noise between the subcarriers and ASE noise is frequency-dependent [12], and this result in tilt SNR in Figs. 3(a) and 4(a).

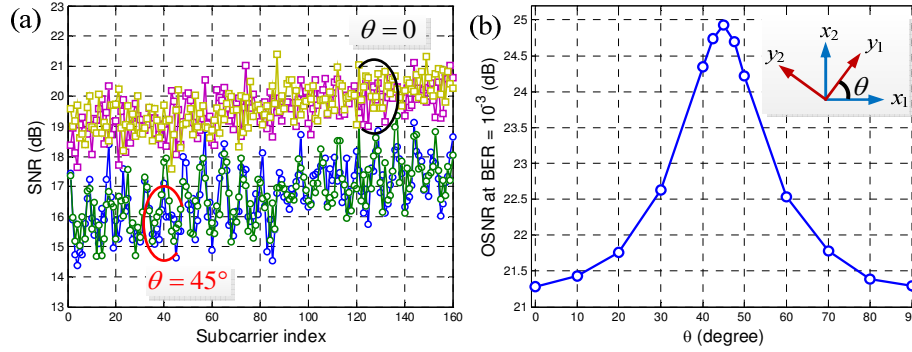


Fig. 3. (a) The received SNR of each subcarrier for $\theta = 0$ and 45° with N_g of 8 and 24-dB OSNR at BtB, and (b) the OSNR at BER of 10^{-3} as a function of θ with N_g of 8 at BtB

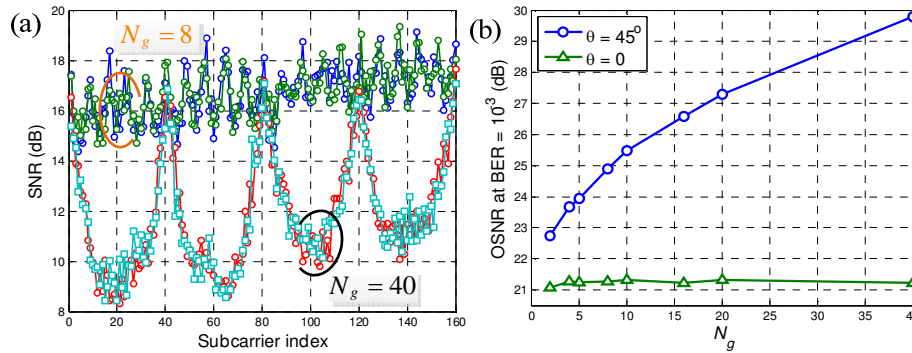


Fig. 4. (a) The received SNR of each subcarrier with N_g of 8 and 40 and 24-dB OSNR for $\theta = 45^\circ$ at BtB, and (b) the required OSNRs at BER of 10^{-3} for $\theta = 0$ and 45° as functions of N_g at BtB.

To evaluate the tolerance to CD of the proposed DD-PDM-OFDM, Fig. 5(a) depicts the BER curves with and without the CD of 16×10^3 ps/nm equivalent to 1000-km single-mode fiber transmission. Compared with the cases at BtB, the BER curves show negligible OSNR penalties after transmission for both θ of 0 and 45° . Furthermore, the effect of DGD on the required OSNR is illustrated in Fig. 5(b), where the dashed curves are the cases with only 16×10^3 -ps/nm CD and the solid curves represents the cases with 16×10^3 -ps/nm CD and 300-ps DGD. While θ is fixed at 0 or 45° , the required OSNRs are evaluated over different relative angles, ϕ , between the PBC and the fiber fast axis. Because DGD would induce frequency-dependent polarization rotation, the performance with θ of 0 might be worse than that with θ of 45° . In fact, the signal performance depends on how the PBS splits the reference carriers, and coexistence of both carriers after the PBS will result in higher condition number. Thus, the results of Fig. 5(b) rely on how the DGD rotates the SOP of the reference carriers. When ϕ is $\sim 22.5^\circ$, for instance, the best case with θ of 0 turns into the worst case. Nonetheless, from Fig. 5(b), the DGD does not contribute additional penalty except polarization mixing, since all the required OSNR are between those in the DGD-free cases with θ of 0 and 45° .

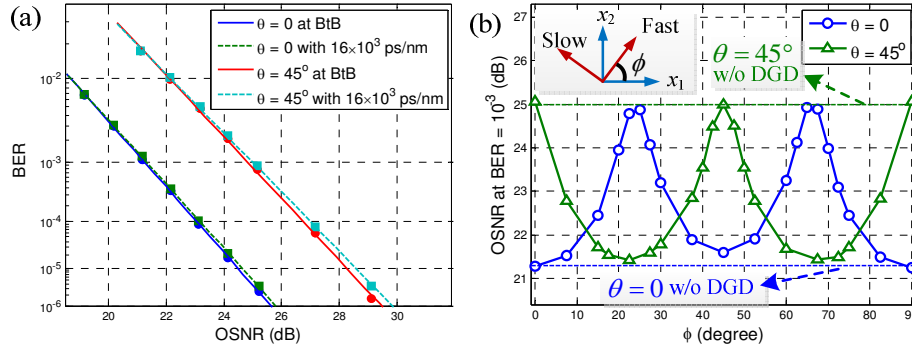


Fig. 5. (a) The BER curves for $\theta = 0$ and 45° with and without 16×10^3 -ps/nm CD, and (b) the required OSNRs at BER of 10^{-3} with 16×10^3 -ps/nm CD and 300-ps DGD as functions of ϕ .

4. Conclusions

In this work, we proposed a novel DD-PDM-OFDM scheme, in which one of the reference carriers' frequencies is shifted to avoid signal fading after transmission. The possible interference among adjacent subcarriers at two SOP can be removed by the proposed MIMO processing. While the performance of the proposed scheme still depends on the SOP of the signals, the OSNR penalty between the best and the worst cases can be suppressed by inserting empty tones among subcarriers. The numerical results show that the maximum OSNR penalty is lower than ~ 3.6 dB with N_g of 8, and it is possible to further decrease this penalty by more empty tones. With the CD of 16×10^3 ps/nm, the proposed 16-QAM 47-Gbps DD-PDM-OFDM signals demonstrate negligible OSNR penalty. Moreover, although PMD would change the received SOP, the simulation results show that the DGD of 300 ps does not induce additional OSNR penalty except polarization rotation. Hence, the proposed scheme is also robust to PMD. In short, compared with a single-polarization DD-OFDM system which suffers from PMD, our PMD tolerant system can increase the spectral efficiency by $\sim 2 \times N_g / (1 + N_g)$, but careful optimization of N_g is needed to maximize capacity owing to the trade-off between the spectral efficiency and the OSNR penalty from polarization mixing.

Acknowledgment

The authors would like to thank the National Science Council, Republic of China, Taiwan for financially supporting this research under Contract No. NSC 100-2221-E-110-089-MY3, NSC 100-2628-E-019-MY3, and NSC 99-2221-E-009 -046-MY3.